

# Heterodyne THz-wave receiver with a superconducting tunneling mixer driven by a high sweeping-speed photonics-based THz-wave local oscillator

Kyoung-Hwan Oh<sup>1a)</sup>, Naofumi Shimizu<sup>1</sup>, Naoya Kukutsu<sup>1</sup>,  
Yuichi Kado<sup>1</sup>, Satoshi Kohjiro<sup>2</sup>, Ken'ichi Kikuchi<sup>2</sup>,  
Takahiro Yamada<sup>2</sup>, and Atsushi Wakatsuki<sup>3</sup>

<sup>1</sup> *Microsystem Integration Laboratories, Nippon Telegraph and Telephone Corporation (NTT)*

*3–1, Morinosato Wakamiya, Atsugi-shi, Kanagawa Pref., 243–0198, Japan*

<sup>2</sup> *Nanoelectronics Research Institute, National Institute of Advanced Industrial Science and Technology (AIST)*

*Tsukuba Central 2, 1–1–1 Umezono, Tsukuba-shi, Ibaraki Pref., 305–8568, Japan*

<sup>3</sup> *Photonic Laboratories, NTT*

*3–1, Morinosato Wakamiya, Atsugi-shi, Kanagawa Pref., 243–0198, Japan*

*a) [ohkh@aecl.ntt.co.jp](mailto:ohkh@aecl.ntt.co.jp)*

**Abstract:** We developed a broadband, highly sensitive heterodyne THz-wave receiver with a superconductor-insulator-superconductor (SIS) mixer. To fully utilize wide-bandwidth characteristics of the SIS mixer, we pump the SIS mixer with a photonics-based local oscillator (PLO) with fast frequency-sweeping speed. The received THz-wave signal down-converted to an intermediated frequency band is rapidly acquired by a high-speed analog-to-digital converter. The noise level of the developed receiver is equal to or smaller than twenty times the quantum-limited noise level between 225 and 425 GHz. With this receiver, the frequency sweep from 225 to 475 GHz with frequency resolution of 0.5 GHz takes only about 2.5 sec. Emission spectra of N<sub>2</sub>O gases measured with this receiver show its excellent performance.

**Keywords:** heterodyne receiver, SIS mixer, photonics-based local oscillator, emission spectroscopy

**Classification:** Microwave and millimeter wave devices, circuits, and systems

## References

- [1] S. Kohjiro et al., “An Octave Bandwidth SIS Mixer for Accurate and Com-

- pact Terahertz Spectrometers,” *IEEE Trans. Appl. Supercond.*, vol. 17, no. 2, pp. 355–358, June 2007.
- [2] A. Wakatsuki et al., “High-power and broadband sub-terahertz wave generation using a J-band photomixer module with rectangular-waveguide output port,” *Conf. Digest of IRMMW-THz 2008*, M4K2, 1199, 2008.
- [3] S. Kohjiro et al., “A 0.2–0.5 THz Single-Band Heterodyne Receiver Based on a Photonic Local Oscillator and a Superconductor-Insulator-Superconductor Mixer,” *Appl. Phys. Lett.*, vol. 93, pp. 093508 1–3, Sept. 2008.
- [4] H. M. Pickett et al., “Submillimeter, millimeter, and microwave spectral line catalog,” *J. Quant. Spectrosc. & Rad. Transfer*, vol. 60, pp. 883–890, 1998.

## 1 Introduction

A heterodyne receiver with a broadband superconductor-insulator-superconductor (SIS) mixer [1] has potential for use as a highly sensitive wide-band THz-wave receiver. However, the bandwidth of a heterodyne receiver is limited by that of the local oscillator (LO), and it is therefore difficult to exploit the wide bandwidth of the SIS mixer. In this study, we introduced a photonics-based THz-wave local oscillator (PLO) that has a wide tuning range, low noise, and fast sweeping speed. The frequency of the PLO can be swept with a sweep speed of 375 GHz/s. In order to follow the fast sweeping speed of the PLO, a delta-sigma based analog-to-digital (A/D) converter was employed in an intermediate frequency (IF) circuit. As a result, a sweeping time as small as 2.5 seconds is realized with an operation frequency ranging from 225 to 475 GHz with a frequency resolution of 0.5 GHz, while maintain the receiver’s high sensitivity. To test the performance of the developed receiver, we measured emission spectra of gas molecules. The results demonstrate the superior performance of the developed THz-wave receiver.

## 2 Receiver components

### 2.1 SIS mixer

We have developed a SIS mixer based on a niobium/aluminum-oxide superconducting junction [1]. The SIS mixer consists of a distributed array of eight superconducting junctions, a twin-slot antenna, and a three-stage transformer as shown in the inset of Fig. 1. Both the THz-wave signal (blue arrow) to be measured and the THz-wave local-oscillator signal (green arrow) are quasi-optically coupled to the SIS mixer chip through a coupler and a lens in front of the window of the cryostat as shown in Fig. 1. The chip is cooled to 4.2 K in a liquid helium cryostat.

### 2.2 PLO

The PLO is based on two-mode beating of optical signal using two wavelength-tunable laser sources (TLSs) operating around 1.55  $\mu\text{m}$  and a uni-traveling-carrier photodiode (UTC-PD) module. The wavelength of one TLS (TLS1)

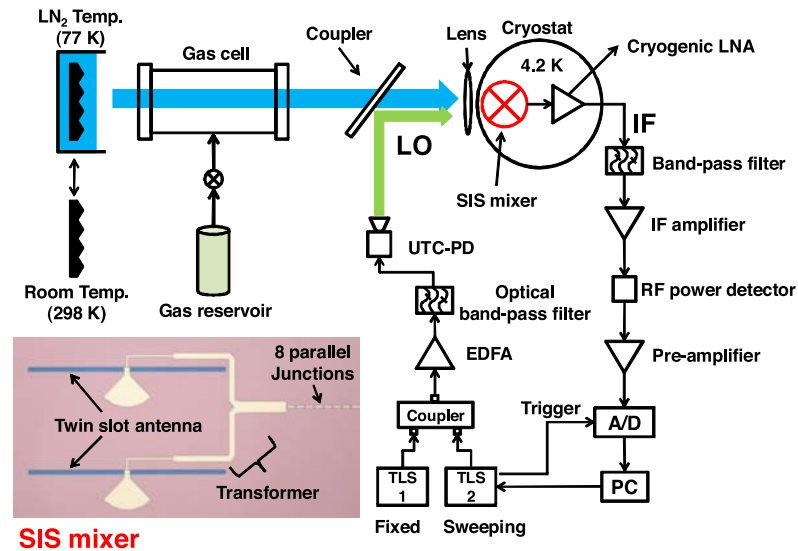


**Fig. 1.** Schematic diagram of a passive gas-spectrum-measurement setup with a SIS mixer and a photoincs-based THz-wave local oscillator.

is fixed at 1548.2 nm, while the wavelength of the other TLS (TLS2) is swept from 1546.4 to 1544.4 nm. The corresponding frequency of the beat signal starts from 225 GHz and stops at 475 GHz. The outputs of TLS1 and 2 are combined with 3-dB coupler and amplified by an erbium-doped fiber amplifier (EDFA). After amplified spontaneous emission noise generated in the EDFA is eliminated with an optical band-pass filter, the optical beat signal is fed into the UTC-PD module [2]. Its maximum output power is 400 and 50  $\mu$ W at 350 and 500 GHz, respectively. The developed PLO can sweep a wide bandwidth of 225 to 475 GHz with a sweep speed of 375 GHz/s. The linewidth  $\delta f \sim 10$  MHz and the frequency accuracy  $\sigma f \sim 100$  MHz of the present PLO's output are dominated by the mutual frequency stability of the two TLSs.

## 2.3 IF circuit

The received THz-wave signal is directly down-converted by the SIS mixer and a signal from the PLO to IF having a frequency of several hundred megahertz. The output signal of the SIS mixer is boosted by a cryogenic low-noise amplifier. After that, a band-pass filter determines the detection frequency range, which is 250 to 750 MHz. A RF power detector detects the power of the IF signal, and then the output of the RF power detector is boosted by a low-noise pre-amplifier. Finally, the voltage of the pre-amplifier output is measured by an A/D converter. To follow fast frequency sweeping speed of the PLO, we used a high-speed A/D converter based on a delta-sigma structure. Its maximum sample rate and A/D resolution are 50 kS/s and 24 bits, respectively. TLS2 provides a trigger signal at each frequency point with a frequency step of 500 MHz. Simultaneously the A/D converter acquires signals with two channels. Channel 1 is connected with the trigger signal from the TLS2 and channel 2 is connected with the output of the

pre-amplifier as shown in Fig. 1. In the two channels, a total of  $66.7 \times 10^3$  sampled points are acquired for one sweep.

Here, we estimate the integration time of the signal measurement at each frequency point. The operation of the A/D converter is synchronized with a master clock of 12.8 MHz, which is generated by an internal crystal oscillator. The A/D converter operates with a sampling rate of 50 kS/s, which corresponds a sample interval of  $20 \mu\text{s}$ . During the sample interval, the A/D converter is controlled with 256 clocks, which are determined by the master clock. The duration of one clock is 78.125 ns. An integration to acquire one sampling point is carried out during a period of two clocks in every four clocks, i.e., the integration time for one sample point is  $2 \times 78.125 \times (256/4) = 10 \mu\text{s}$ . To obtain the signal at each frequency point, 17 sampled points are averaged. The center point of the 17 sampled points corresponds to a trigger signal. The eight points before the center point and the eight points after it are positioned before and after the corresponding trigger point. Thus, the integration time of the signal measurement at each frequency point for one sweep can be regarded as seventeen times the integration time for one sample point, i.e.,  $(8 \times 2 + 1) \times 10 = 170 \mu\text{s}$ . This integration corresponds to 127.5 MHz of the frequency window for each frequency point. The pre- and post-processing take about 0.9 and 0.9 sec, respectively, on a PC. Therefore, it takes about 2.5 sec to show the 225- to 475-GHz spectrum in one sweep.

### 3 Receiver performance

The receiver noise temperature  $T_{\text{RX}}$  was measured by the conventional Y-factor method, where  $T_{\text{RX}}$  is derived from the ratio of the IF output power for the hot (298 K) antenna load to the cold (77 K) ones. To evaluate the performance of the PLO, its  $T_{\text{RX}}$  was compared with the  $T_{\text{RX}}$  of conventional multiplier-based CW oscillators driven by a microwave synthesizer or Gunn diodes. Fig. 2 shows noise temperature characteristics of two kinds of LO. Red dots show the  $T_{\text{RX}}$  measured when the SIS mixer was driven by the PLO, black stars replot the  $T_{\text{RX}}$  of the conventional multiplier-based LOs from [3], and the black line is twenty times quantum-limited noise level in a frequency range of 225 to 475 GHz. The result demonstrates that the PLO does not produce any remarkable additional noise in compared with the conventional multiplier-based LOs, except in the frequency regions below 275 GHz and above 425 GHz. In these regions, the power uncertainty at the base line is larger than that in a frequency range of 275 to 425 GHz. Noise temperature less than twenty times the quantum-limited noise level is achieved in the bandwidth of 57% of the center frequency. Fig. 2 also indicates the clear difference in the bandwidth between the PLO and the conventional LOs. The PLO covers 225 to 475 GHz completely, while the three conventional LOs with different frequency band cover a part of this band (arrows). Notably, the  $T_{\text{RX}}$  measurement of the PLO can be carried out with fast frequency sweeping of 375 GHz/s, while that in the conventional case is done at each fixed frequency. This advantage of the PLO makes it

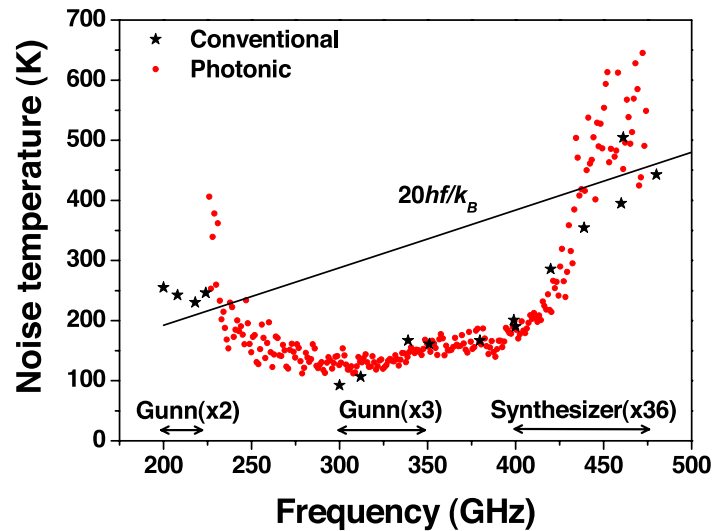


Fig. 2. Receiver noise temperature  $T_{RX}$  vs. frequency.

possible to dramatically reduce the measurement time over a wide frequency range, which is indispensable for accurate spectrum measurement.

#### 4 Emission spectroscopy of $N_2O$

To demonstrate the high sensitivity and wide bandwidth of the developed receiver, we carried out passive gas spectrum measurements with  $N_2O$  gas. A gas cell with the length of 0.2 m was positioned between the cryostat window and the thermal radiator as shown in Fig. 1. The cell was filled with  $N_2O$  gas diluted by  $N_2$  with the concentration of 100, 66, or 33% and the pressure of  $\sim 1000$  hPa. The gas spectrum was detected by positioning a 77-K thermal emitter at the background of the gas cell, soon after the detected power had been calibrated with the 77- and 298-K emitters at the back of an empty gas cell. In this measurement, a fast frequency sweep from 225 to 475 GHz was carried out sixteen times and then the spectra for all sweeps were averaged.

Fig. 3 shows the measured THz-wave emission spectra of  $N_2O$  gases at room temperature. As shown, the emission peaks with a  $\sim 0.1$ -pW amplitude and 25-GHz interval, which is specialized for  $N_2O$ , were successfully detected. Theoretical emission intensities of  $N_2O$  molecules in a 0.2-m gas cell at room temperature are 0.33, 0.20, and 0.12 pW for the 100-%, 66-%, and 33-%  $N_2O$  at 352 GHz, respectively [4]. The theoretical estimations agree very well with the measurement results as shown in Fig. 3.

Based on the Dicke radiometer equation, the root-mean square uncertainty of the brightness temperature  $\delta T_{RMS}$  and corresponding minimum detectable power of the receiver are defined  $\delta P_{RMS}$  as

$$\delta T_{RMS} = \frac{T_{RX} + T_{ANT}}{\kappa \sqrt{B \cdot \tau}} \quad (1)$$

and

$$\delta P_{RMS} = k_B B \delta T_{RMS}, \quad (2)$$

respectively, where  $T_{\text{ANT}}$  is the radiation temperature of the antenna load,  $\kappa$  is the coupling efficiency between the receiver and the object being measured,  $B$  is the final detection bandwidth, and  $\tau$  is the total signal integration time. For  $T_{\text{RX}} = 150 \text{ K}$ ,  $T_{\text{ANT}} = 77 \text{ K}$ ,  $\kappa = 1$ ,  $B = 0.5 \text{ GHz}$ ,  $\tau = 170 (\mu\text{s}) \times 16$ , one finds the theoretical power resolution of  $\delta P_{\text{RMS}} = 1.4 \text{ fW}$ . The minimum detectable power evaluated from the experimental result is about 5–10 fW. The discrepancy might be attributed to the fluctuation of receiver gain during the multiple sweeps. Optimizing the number of averagings will reduce the discrepancy in  $\delta P_{\text{RMS}}$  between the experiments and theory.

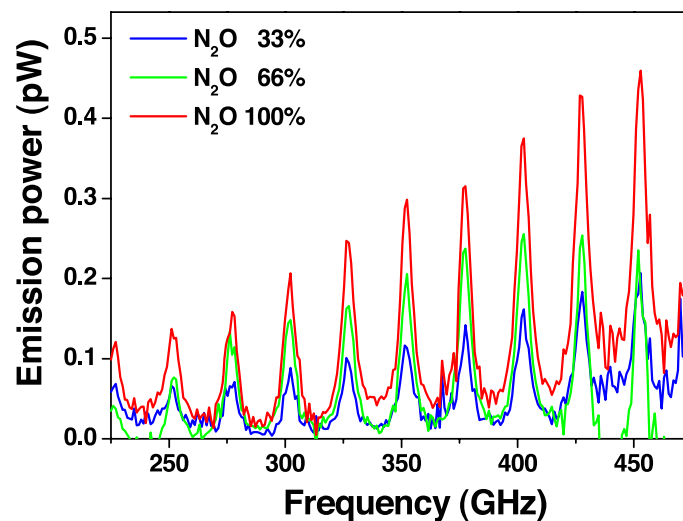


Fig. 3. Measured spectra of  $\text{N}_2\text{O}$  of 33, 66, and 100%.

## 5 Conclusion

A broadband, highly sensitive heterodyne receiver has been developed. To exploit the wide-bandwidth characteristics of the SIS mixer in this receiver, we pump the SIS mixer with a PLO with the frequency-sweeping speed of 375 GHz/s between 225 and 475 GHz. In addition, a high-speed A/D converter was introduced in the IF circuitry of the receiver to follow the high-sweeping speed of the PLO. This single-band receiver, which fully covers 225 to 475 GHz and exhibits a noise temperature less than twenty times quantum-limited noise in the bandwidth of 57% of the center frequency, takes only about 2.5 sec for one sweep with the frequency resolution of 0.5 GHz. Emission spectra of  $\text{N}_2\text{O}$  gases measured with this receiver show its excellent performance.

## Acknowledgments

This work was supported in part by the National Institute of Information and Communications Technology (NICT), Japan. Kyoung-Hwan Oh thanks Mr. Changkyo Lee of ICU in the Republic of Korea for fruitful discussions about the principle of a delta-sigma analog-to-digital converter's operation.